Journal of Materials Chemistry B

ROYAL SOCIETY OF CHEMISTRY

PAPER

View Article Online
View Journal | View Issue

Cite this: J. Mater. Chem. B, 2025, 13, 4671

Bioinspired hybrid DNA/dendrimer-based films with supramolecular chirality†

Rita Castro, [a] Pedro L. Granja, [bc] João Rodrigues, [a] Ana Paula Pêgo [bcd] and Helena Tomás *[a]

Received 12th December 2024,
Accepted 11th March 2025

DOI: 10.1039/d4tb02761b

rsc.li/materials-b

Bioinspired hybrid DNA/dendrimer films were obtained by heating long double-stranded DNA (dsDNA) above its melting temperature and, while in the denatured state, mixing it with poly(amidoamine) (PAMAM) dendrimers, followed by controlled cooling. The formation of these new types of films was found to be dependent on several parameters, including the initial heating temperature, pH, buffer composition, dendrimer generation, amine/phosphate (N/P) ratio, and cooling speed. In addition to the PAMAM dendrimers (generations 3, 4, and 5), films could also be produced with branched poly(ethylenimine) with a molecular weight of 25 kDa. The results indicated that these films were formed not only through electrostatic interactions established between the negatively charged DNA molecules and the positive dendrimers, as expected, but also through random rehybridization of the single-stranded DNA (ssDNA) during the cooling process. The resulting films are water-insoluble, transparent when thin, highly elastic when air-dried, exceptionally stable over extended periods, cytocompatible, and easily scalable. Notably, the slow cooling process allowed for the establishment of at least a partially ordered structure in the films, as revealed by circular dichroism, providing evidence of supramolecular chirality. It is envisioned that these films may have significant potential in biomedical applications, such as drug/gene delivery systems, platforms for cell-free DNA transcription and components in biosensors.

Introduction

Dendrimers may be regarded as a special type of branched polymer that grows radially from a central core, layer by layer, increasing their generation each time a layer is built.[1,2] They differ from classical polymers in their characteristics and well-defined architecture, size, shape, and controlled number of terminal groups. Poly(amidoamine) (PAMAM) dendrimers, which have an ethylenediamine (EDA) core with tertiary amines at the branching points and terminal primary amines, were initially synthesized by Tomalia *et al.* in the 1980s.[3,4] These multivalent molecules display a number of terminal groups that increase exponentially with each generation ($2n + 2$, where "n" is the generation number).[5] Depending on the solution's pH value, PAMAM dendrimers may present different protonation degrees, resulting in conformational changes.[6,7] The pK_a is in the range of 3 to 6 for the internal tertiary amines, and from 7 to 9 for the terminal primary amines.[5] Consequently, at a very high pH (pH $>$ 10), PAMAM dendrimers are non-charged. They become slightly cationic at a near-neutral pH (pH $\simeq$ 7) due to the protonation of the primary amines and finally form very strongly cationic polymers at a low pH (pH $<$ 6) due to the full protonation of the tertiary amines. This characteristic of PAMAM dendrimers opened the possibilities for their use as vehicles to deliver genetic material into cells. Indeed, a vast body of work shows that cationic dendrimers can interact with anionic RNA or DNA molecules, neutralizing their charge and serving as condensing and transfection agents.[8–12] The use of dendrimers in nucleic acid delivery was based on their resemblance to histones, the proteins that condense DNA in the nucleus of eukaryotic cells to form the chromatin.[13] Histones, highly basic proteins, establish several distinct interactions with DNA (*e.g.*, electrostatic forces, hydrogen bonds, and non-polar interactions) that together overcome the energy barrier for compaction.[14,15] Approximately 147 base pairs (bp) of DNA are wrapped around a group of 8 positively charged histones (histone octamer) in a left-handed superhelix to form a nucleosome core particle.[16] Each nucleosome is then connected to the next by linker DNA, forming a linear array of nucleosomes, a structure known as the "beads-on-a-string" that constitutes chromatin.[15] In fact,

[a] CQM-Centro de Química da Madeira, MMRG, Universidade da Madeira, Campus da Penteada, 9020-105 Funchal, Portugal. E-mail: lenat@staff.uma.pt
[b] Instituto de Investigação e Inovação em Saúde (i3S), Universidade do Porto, 4200-135 Porto, Portugal
[c] Instituto de Engenharia Biomédica (INEB), Universidade do Porto, 4200-135 Porto, Portugal
[d] Instituto de Ciências Biomédicas Abel Salazar (ICBAS), Universidade do Porto, 4050-343 Porto, Portugal

† Electronic supplementary information (ESI) available. See DOI: https://doi.org/10.1039/d4tb02761b

chromatin has been shown to be not only a highly complex biological structure but also a dynamic one that responds to environmental changes, and dendrimers have been used as models to study DNA–histone interactions.[17]

Inspired by nature and exploring the distinctive interactions between dendrimers and nucleic acids, this work introduces a novel approach to the preparation of DNA-based films. The idea was to subject long DNA to temperatures exceeding its melting temperature (T_m), inducing its denaturation and formation of single-stranded DNA (ssDNA). Then, while keeping the denatured DNA molecules at high temperature and before allowing a slow cool down, introduce dendrimers into the system. Under strict experimental conditions, the application of this methodology resulted in the formation of soft 2D films composed of DNA and dendrimers, which exhibited at least partial internal ordering, as indicated by circular dichroism analysis. Herein, we present the optimized conditions for the preparation of these films, as well as the characterization of the end materials. By exploring different experimental conditions, insights into the type of interactions responsible for film formation were obtained, which may also be valuable for understanding other DNA-based constructs, including natural or biomimetic systems such as the previously mentioned nucleosome arrays in chromatin.

Results and discussion

Optimal experimental conditions for film formation

Hybrid DNA/dendrimer-based films were successfully prepared following the strategy depicted in Fig. 1 and using PAMAM dendrimers of generation 3 (G3), 4 (G4) and 5 (G5). An optimal experimental protocol was first established, which involved long dsDNA ($\simeq$ 12 kbp, as determined by agarose gel electrophoresis, ESI,† Fig. S1). In this context, dsDNA was initially dissolved in phosphate-buffered saline solution (PBS, without Ca^{2+} and Mg^{2+}) and the pH was adjusted to 6. After heating the dsDNA to 99 °C to promote denaturation into ssDNA (above its T_m of 87.5 °C), a determined volume of the specific dendrimer solution was added, and the two oppositely charged polymers were left to interact for a few minutes. Following this, the solution underwent a slow cooling process to room temperature using a controlled temperature ramp (CTR: 99 °C (5 min) → 87 °C (5 min) → 68 °C (5 min) → 50 °C (5 min) → 24 °C (5 min) → room temperature), allowing sufficient time for the system components to organize. Thin and homogeneous films were always formed at the bottom of the tube, which could be removed using a micropipette tip and easily characterized (ESI,† Movie). These films could be prepared at N/P ratios ranging from 3 to 5, where the N/P ratio represents the molar ratio between the number of primary amine groups in the dendrimers and the number of phosphate groups in the DNA. An illustrative example of the optimized protocol used for film preparation is shown in detail in the ESI,† Fig. S2, beginning with 500 μg of dsDNA and using G3 PAMAM dendrimers at an N/P ratio of 4.

Confirmation of dendrimers and DNA presence in the films

Experiments were conducted to visually confirm the actual presence of DNA and dendrimers in the film structure. To verify the presence of DNA, the films were immersed in a solution of ethidium bromide, a fluorescent molecule that intercalates between the base pairs of DNA. Upon contact with the solution, the DNA gradually became stained and showed a pale pink/orange colour (Fig. 2a), while the solution itself gradually lost its colour. When exposed to UV light, these films exhibited fluorescence in the orange range (Fig. 2b). The presence of dendrimers in the films was confirmed using rhodamine-functionalized dendrimers (Fig. 2c) as part of the film preparation process (see details of the functionalization process in the ESI,† Fig. S3). Under green light illumination, these films emitted a bright orange/red fluorescence characteristic of the rhodamine dye

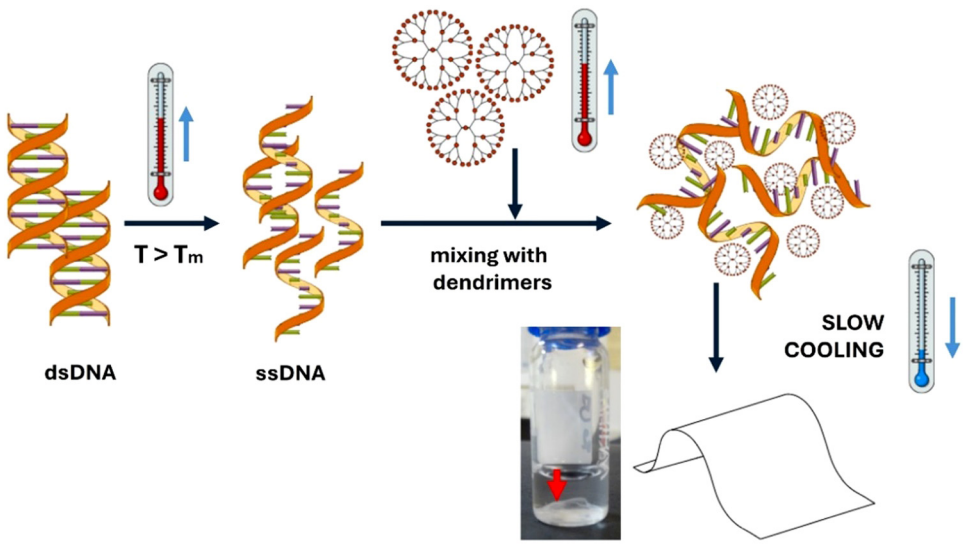

Fig. 1 General strategy followed for the preparation of hybrid DNA/dendrimer-based films. The dsDNA and dendrimers are first heated separately above the dsDNA melting temperature (T_m), then mixed, and subsequently subjected to a slow cooling process.

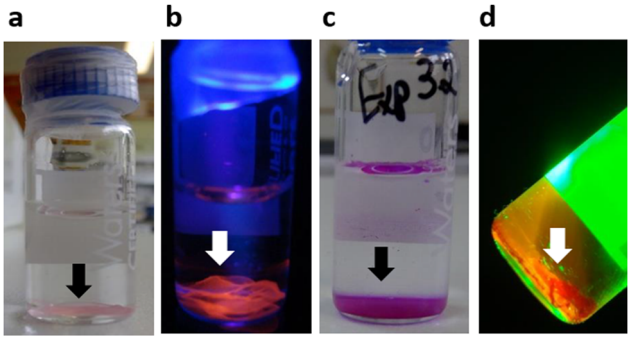

Fig. 2 Films prepared with G4 PAMAM dendrimers at an N/P ratio of 5 in the bottom of glass vials. DNA presence was confirmed by ethidium bromide staining: (a) films showing a pale pink/orange color; (b) films showing strong orange fluorescence under blue light irradiation. The presence of dendrimers was confirmed using rhodamine-functionalized dendrimers during film preparation: (c) films showing a pink/purple color; (d) films showing bright orange fluorescence under green light irradiation. The arrows point to the films on the bottom of the flasks.

(Fig. 2d). Moreover, the DNA content in freshly prepared films was indirectly quantified by spectrophotometry (absorbance at 260 nm) using the supernatant, revealing a very high DNA incorporation efficiency, namely 97.7 ± 0.6%, 97.8 ± 0.3% and 98.5 ± 0.4%, for films prepared at an N/P = 4 with G3, G4 and G5 dendrimers, respectively.

Impact of several experimental parameters on film formation

Studies on the effect of different experimental conditions on the successful preparation of the hybrid DNA/dendrimer-based films allowed for a comprehensive understanding of the underlying processes and the nature of the interaction between DNA and PAMAM dendrimers. These parameters included the maximum temperature applied (for dsDNA melting), the ionic composition of the dsDNA solution, the cooling program, the DNA concentration, the initial pH of the dsDNA solution and the N/P ratio, the dendrimer generation and the use of other polymers with varying molecular structures and weights.

(a) Effect of the maximum temperature applied. To understand the importance of the extent of dsDNA denaturation for film formation, several experiments using G5 dendrimers were performed where dsDNA was initially heated at temperatures of 25, 50, 68, 87 or 99 °C. For each case, assays were performed for several N/P ratios (from 0.5 to 15) while keeping constant all other parameters. Film formation was only observed when the DNA solution was heated up to 99 °C, a temperature higher than its T_m, and at N/P ratios in the range 3–5. These results show that DNA denaturation needs to occur to a high extent for successful film formation.

(b) Effect of ionic composition of DNA's solution. Attempts to prepare DNA/dendrimer films were made using media with different ionic compositions, namely ultrapure water, 0.15 M NaCl, Tris-ethylenediaminetetraacetic acid buffer (Tris-EDTA), and PBS solution (without Ca^{2+} and Mg^{2+}). Regardless of the dendrimer generation, film formation only took place using PBS solution. Since the initial pH of the DNA solution was always kept constant (pH = 6), the influence of ionic strength and composition on the process can be compared. In terms of ionic strength, both water and TE buffer present lower values than PBS solution. However, the ionic strength is nearly the same for both 0.15 M NaCl and PBS solution, meaning that this parameter is not the only one affecting film formation. Indeed, based on these assays, it can be concluded that the composition of the solution is of key importance. Indeed, Kéri *et al.* drew attention to the interactions established between PAMAMs and the phosphate ions present in the PBS solution.[18] They concluded that around neutral pH (pH = 5–8), phosphate ions were not only incorporated into PAMAM dendrimers by forming hydrogen bonds with the tertiary amines, leading to a decrease in the dendrimer's hydrodynamic diameter, but also interacted with the primary amines at the dendrimer's periphery. Given this fact, since $H_2PO_4^-$ is the dominant phosphate ion in the PBS solution at pH 6, the possibility of it acting as a bridge leading to the formation of dendrimer aggregates was also suggested by the authors.[18] Therefore, with this in mind, phosphate ion-mediated dendrimer interactions can be a crucial step for DNA/dendrimer-based film formation, even if this may not necessarily involve the establishment of stable dendrimer aggregates in solution. These results can be explained by the cooperative binding of dendrimers to DNA found by several authors.[19,20] In these studies, DNA/dendrimer complexes were found to coexist with free DNA molecules when both entities were mixed, revealing the preferential attachment of dendrimers to DNA/dendrimer complexes compared to free DNA. This is especially noticeable for low N/P ratios. Possibly, the presence of phosphate ions facilitates this cooperative binding process by helping to bring the dendrimers closer.

Moreover, the addition of $MgCl_2$ at a very low concentration (0.5 mM) to the standard PBS solution prevented film formation, although the change in ionic strength was minimal. In fact, divalent Mg^{2+} ions are known to interact with the phosphate groups present in the DNA backbone, increasing double helix stability and the T_m value.[21] Yet, agarose gel electrophoresis studies showed that the possible increase in T_m promoted by the presence of Mg^{2+} ions was not sufficient to impair the melting of DNA when 99 °C was applied, nor its partial hybridization upon controlled cooling (ESI,† Fig. S4). Hence, the shielding of DNA's negative charge and the decrease in interaction with the dendrimers should explain the impairment of film formation in the presence of the Mg^{2+} ions. Again, the importance of the electrostatic interactions between DNA and dendrimers is evidenced.

(c) Effect of the cooling program. The cooling program also played a decisive role in film formation. A fast-cooling procedure, either by leaving the mixtures to cool at room temperature (RT) or by immersing them directly in an ice bath after heating to 99 °C, prevented film formation. In contrast, a slow cooling program was effective. These results indicate that the molecules in the mixture need time to form the film, suggesting the potential presence of an internal organization within the material. Agarose gel retardation studies showed that when DNA alone was heated until denaturation and then fast cooled,

almost all DNA remained as ssDNA (ESI,† Fig. S5). Under CTR cooling, dsDNA was detected but remained in the well; that is, the ssDNA molecules hybridized randomly, resulting in a cross-linking process. Interestingly, no dsDNA was detected when dendrimers were mixed with DNA at RT or after being heated to 99 °C and then cooled (regardless of the cooling program). This likely means that DNA underwent compaction in the presence of dendrimers, thus inhibiting EtBr intercalation. In summary, the slow cooling program applied during film preparation facilitated DNA hybridization (at least partially between the free ssDNA segments), while the dendrimers acted as compaction agents.

(d) Effect of the initial pH of the DNA solution and of the N/P ratio. The influence on film formation of the initial pH of the DNA solution was evaluated by adjusting pH values to 5, 6, 7 or 8 prior to the heating step. Attempts to prepare films were then made at each pH value using G3, G4 and G5 PAMAM dendrimers at different N/P ratios, and information on whether films were obtained was recorded (Table 1). It is important to note that film formation was confirmed visually, requiring the film to be mechanically resistant enough to be detached from the bottom of the tube in one piece.

First, results showed that stable films were only formed when adjusting the initial pH to 6, regardless of the dendrimer generation or the N/P ratio. Second, at a pH of 6, film formation was restricted to three N/P ratios, namely 3, 4, and 5, regardless of the dendrimer generation. Therefore, it seems that film formation depends on the one hand on the initial global protonation level of the dendrimers in solution (determined by the initial pH of 6), and on the other hand, on the charge density associated with the individual dendrimers which is affected by the N/P ratio. Indeed, since the amount of DNA is kept constant, low N/P ratios correspond to fewer dendrimers in solution, whereas high N/P ratios correspond to a greater number. Thus, considering that the total number of protonated amines in solution remains constant at a given pH, the dendrimer's charge density is expected to be higher at lower N/P ratios and *vice versa*. An optimal positive charge density in the dendrimers is therefore required to achieve the right electrostatic conditions for film formation.

Table 1 Effect of the initial pH of the DNA solution on film formation, in combination with the effects of the N/P ratio and dendrimer generation (Gx). Film formation was confirmed visually, requiring the film to be mechanically resistant enough to be detached from the bottom of the tube in one piece (n = 3)[a]

Initial pH	Gx	N/P ratio 1	2	3	4	5	6	7	8	9	10
5.0	G3	Clear solution									
	G4										
	G5										
6.0	G3			STABLE FILM WAS FORMED			Quasi-film was formed				
	G4										
	G5										
7.0	G3	Fine/coarse precipitate was formed									
	G4										
	G5										
8.0	G3	Clear solution									
	G4										
	G5										

[a] A quasi-film refers to a continuous layer of material that cannot be removed from the tube without breaking into fine particles.

(e) Effect of the DNA concentration and size. The experiments described until now used a DNA solution of 1 mg mL^{-1}. Maintaining all other conditions constant and using G5 PAMAM dendrimers, a set of assays was made varying the DNA concentration in solution (0.2, 0.6, 1.0 and 2.0 mg mL^{-1}) and, for each concentration, varying the N/P ratio. Results showed that the range of N/P ratios allowing film formation shifted to higher values when the DNA concentration was low and *vice versa*. For DNA concentrations of 0.2 mg mL^{-1} and 0.6 mg mL^{-1}, films were formed within the N/P ratio range of 7.5–10.0 (although they were very thin and fragile). At a DNA concentration of 1.0 mg mL^{-1}, films were formed within the N/P ratio range of 3.0–5.0, while at a DNA concentration of 2.0 mg mL^{-1}, films formed within an N/P ratio range of 2.5 to 5.0. These results are consistent with the idea that a higher number of dendrimer molecules are needed to form a film if the DNA molecules are further apart in solution, that is, dendrimer crowding reveals to be important in the process.

Also, during the course of the work, unsuccessful attempts were made to prepare the films using the 12 kbp dsDNA after subjecting it to sonication for different durations (ranging from 10 to 70 minutes). Since sonication causes DNA fragmentation, it was concluded that the DNA molecule size is crucial for film formation, most likely due to the extent of DNA rehybridization required in the process. That is, the DNA must be sufficiently long to, on the one hand, interact with the dendrimers and, on the other hand, contain chain segments capable of rehybridizing to ensure the spatial continuity of the films.

(f) Effect of dendrimer generation (low generation dendrimers). While films could be prepared from G3, G4, and G5 dendrimers, attempts to formulate them with lower dendrimer generations (G1 and G2) were unsuccessful. It has been reported that while the higher generations tend to adopt a spherical shape, the lower ones are more planar structures, a characteristic that undoubtedly affects their spatial charge distribution.[7,22] Indeed, distinct behaviour among dendrimer generations regarding DNA compaction has often been shown for both ssDNA and dsDNA.[23,24] It is well-established that higher generations are significantly more efficient in DNA condensation, a finding not only based on experimental work but also on computational chemistry studies.[25–28] For example, a systematic study by Qamhieh *et al.* on the interaction of dsDNA with different PAMAM generations showed that the

number of DNA turns around a dendrimer increases with the generation and that the DNA/dendrimer complexes can adopt different morphologies such as rods, toroids, or globular aggregates.[28] They also concluded that complexes with G1 PAMAM dendrimers were not stable as their charge was not sufficient to neutralize the DNA. In addition, as discussed before, the inability to obtain films with small-generation dendrimers may also be related to the fact that they are expected to establish weaker interactions with phosphate ions in solution, making dendrimer proximity mediated by these ions less likely. Overall, low-generation PAMAMs have a smaller overall positive charge and differences in shape, size, and charge density, which can interfere with their interaction with nucleic acids, resulting in structures that are not favourable for film formation.[7,29]

(g) Use of other cationic polymers. After successfully preparing DNA/dendrimer-based films and for a better understanding of their nature, we tried to use other cationic polyelectrolytes for the same purpose. The idea was to assess whether the architecture of the polymers (linear or branched) and their size/molecular weight (MW) were crucial parameters for film formation. Thus, we began by attempting to prepare films using poly(ethyleneimine) (PEI) of three types: 0.8 kDa branched PEI, 25 kDa branched PEI and 10 kDa linear PEI. Experiments showed that when 0.8 kDa branched PEI was used, the mixture resulted in clear solutions. In fact, its MW is lower than that of G1 PAMAM (1.4 kDa), for which films also did not form. In contrast, a stable film was achieved using 25 kDa branched PEI (DNA incorporation efficiency was 99.3 ± 0.1%) which has a MW comparable to the G5 PAMAM dendrimer (28.8 kDa) and approximately 200 primary amine groups per molecule (theoretically, the G5 PAMAM has 128 amine groups at the surface and 126 additional tertiary amines in its interior). For the 10 kDa linear PEI, which has a MW between that of G3 (6.9 kDa) and G4 (14.2 kDa) PAMAM dendrimers, also no film could be produced. Instead, the solution became turbid, and a thin layer of white particles was visible in the bottom of the container. In addition to PEI, 56 kDa linear poly(allylamine hydrochloride) and 5 kDa linear chitosan oligosaccharides were also tested. In agreement with the results obtained with PEI, no films were formed in these cases either. In summary, not only the size (and, thus, overall charge of the molecule), but also the existence of primary amines and a spherical (or near-spherical) shape of the molecules seem to be important requirements for the process to be successful. Indeed, for a given volume, a sphere has the smallest surface area. Therefore, for equivalent MW (assuming that volume and MW are proportional), charge will be more concentrated in spherical molecules (branched polymers), resulting in a higher charge density.[30] Thus, these experiments confirm that the charge density of the cationic polymer is an important factor in film formation.

As previously mentioned, dendrimers have been used as models of histones and, in this context, protamine from salmon sperm was also assayed for film preparation. Protamine is an arginine-rich protein known for condensing DNA in sperm, as it strongly binds to and wraps around the DNA helix, forming supramolecular toroid structures.[31] Due to its high content in arginine residues (pK_a = 12.5), protamine is a very basic molecule. It contains many positively charged guanidinium groups that are protonated at pH values lower than its pK_a value.[32,33] Moreover, the binding of protonated arginine residues to DNA's phosphate groups is mainly of electrostatic nature and base-sequence independent, contrary to what happens with histones. When protamine was tested for preparing films with DNA, a very fragile film was formed at the bottom of the tube that could not be removed intact. Indeed, the MW of the used protamine (4.2 kDa) is between those of G2 and G3 PAMAMs, which may explain this result. Another possibility could be temperature-induced denaturation of protamine during the heating step, which may alter its conformation and, consequently, its interaction with DNA, affecting DNA condensation.

Characterization of DNA/dendrimer-based films

(a) Stability over time. The DNA/dendrimer-based films demonstrated a remarkable long-term stability. After a 105-day (3.5 months) incubation in PBS solution (pH 7.4), at 37 °C, films prepared with G3, G4, and G5 dendrimers, at an N/P ratio of 4, released 1.0%, 1.4% and 2.4% of the initial amount of DNA incorporated. Moreover, even when the films were exposed to a PBS solution containing 10% (v/v) foetal bovine serum (FBS) at 37 °C, DNA release remained minimal. After three weeks, despite the presence of nucleases in FBS capable of degrading DNA, less than 4% of the initial DNA content was released from the films (ESI,† Fig. S6). These findings suggest that the DNA is effectively compacted and well-protected within the DNA/dendrimer-based films.

(b) Stability under extreme pH variation. The stability of the DNA/dendrimer-based films under extreme pH values was studied. To achieve this objective, freshly prepared DNA/G5 dendrimer-based films were exposed to concentrated HCl or NaOH solutions, either directly on their surface or in the solution in which they were formed. In all the cases, the films remained intact under strong acidic conditions. However, under strong alkaline conditions, the films dissolved instantaneously and completely, leaving the solutions transparent and colourless. These results confirmed the electrostatic nature of the forces behind film formation. In a very acidic medium, the level of protonation of dendrimers was maintained, and the films remained intact (possibly, the DNA molecules were not degraded because they were protected from the environment after compaction). In contrast, under extreme alkaline conditions, the dendrimers lost their positive charge due to the deprotonation of amines and the films dissolved. In addition, at very high pH values, DNA may undergo denaturation and degradation due to the breaking of hydrogen bonds and backbone cleavage[34] which may also have contributed for film degradation. This process was captured as a movie, under an inverted microscope (ESI,† Movie).

(c) Zeta potential (ZP) of the films' surface. The surface zeta potential of DNA/dendrimer-based films prepared with G3, G4, and G5 dendrimers at an N/P ratio of 4 was measured, showing positive values that were not significantly different

among the three dendrimer generations (24 ± 5 mV, 22 ± 5 mV and 22 ± 12 mV for DNA/G3, DNA/G4 and DNA/G5 dendrimer films, respectively). The positive values were not surprising, given the evident excess of dendrimer in the films (the N/P ratio was above 1) which were protonated at pH 6. Also, since the N/P ratio used was constant, similar ZP values were expected (ESI,† Table S1).

(d) Circular dichroism (CD) studies. The CD technique measures the difference in absorbance (A) of left (L) and right (R) circularly polarized light ($\Delta A = A_L - A_R$) in samples containing one or more chiral groups.[35,36] If a molecule absorbs more left than right circularly polarized light, the CD signal is positive; otherwise, the CD signal is negative. This technique is commonly used to understand protein and DNA structures under different environmental conditions, including in the case of DNA-based films, as DNA is optically active.[37,38] Here, CD measurements were performed on DNA/dendrimer films based on G3, G4, and G5 dendrimers at different N/P ratios. Fig. 3a shows the CD spectra of a 1 mg mL^{-1} DNA solution (the DNA concentration used in film preparation), in the absence of dendrimers, before and after the heating/cooling process. Both spectra correspond to the typical CD spectrum of DNA in the B-form (right-handed helix, medium compacted structure) with a broad positive band at 260–280 nm and a negative band around 245 nm.[37,38] This indicates that the hybridization process occurred without significant changes in DNA's conformation. However, these bands were not observed in the CD spectra of the DNA/dendrimer films, where large positive bands with maximum wavelength values around 300 nm appeared. Fig. 3b shows the CD spectra for films prepared with the G3 dendrimer at N/P ratios of 3, 4, and 5. These bands reached signal intensities that ranged from 35 (N/P = 3) to 70 (N/P = 5) times higher than those at lower wavelengths as observed in Fig. 3a for DNA alone. As seen in the spectra, when G3 dendrimers were used, an increase in the N/P ratio (*i.e.*, when more dendrimers were added) led to increased CD intensity values. Moreover, films prepared at the same N/P ratio with G4 and G5 dendrimer generations (Fig. 3c) showed CD spectra with a similar behaviour. In this case, the intensity of the band with the maximum wavelength at ≃300 nm decreased with an increase in the dendrimer generation. It should be noted that control experiments were carried out with solutions containing only dendrimers or the supernatants of the films (ESI,† Fig. S7), which revealed that the high-amplitude bands present in the CD spectra came from the films themselves.

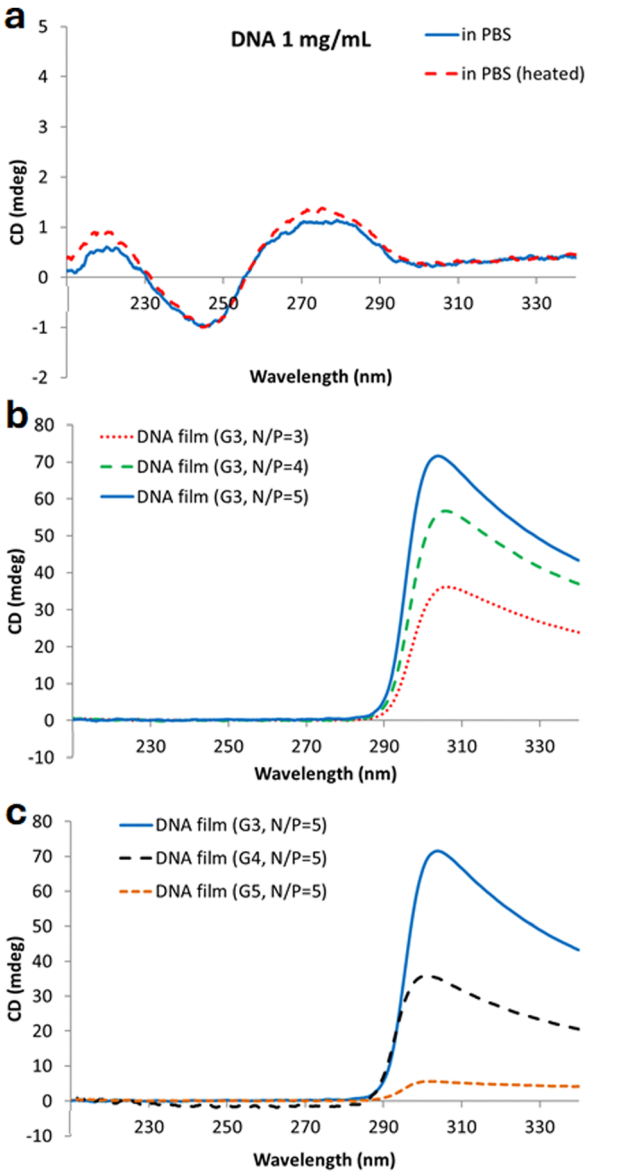

Fig. 3 Circular dichroism (CD) spectra. (a) DNA at 1 mg mL^{-1} before and after the heating/cooling process (CTR), (b) DNA/G3 dendrimer films at different N/P ratios, and (c) DNA/G3, DNA/G4 and DNA/G5 dendrimer films at an N/P ratio of 5. Note that y-axis scales are not the same in all graphs, as the scale in graph (a) is 16-fold lower.

Some literature studies from the 1970s and 1980s, as well as other more recent studies, have reported this type of CD spectra for condensed forms of DNA, such as DNA particles of biological origin (*e.g.*, sperm heads, nucleosomes),[39,40] DNA aggregates produced by several condensing agents (*e.g.*, salts, polymers),[41–43] and cholesteric liquid crystalline dispersions of nucleic acids.[44,45] Originally, these spectra were designated as "psi-spectra", meaning "polymer and salt-induced" CD spectra.[41] Keller and Bustamante analysed these "abnormal" bands in the CD spectra of DNA aggregates and suggested that the anomalously large signals in CD spectra (which can be positive or negative) result from the presence of a long-range chiral structure in the aggregate, together with a "collective response" of the chromophores due to delocalization throughout the entire system of the light-induced excitations.[46] This means that distant parts of the aggregate must be coupled to each other to generate abnormally high CD signals, although the distances in question are small, *i.e.*, comparable to the wavelength of the incident light. Furthermore, based on experimental evidence, they concluded that the contribution of differential scattering to the overall CD signal in this type of system is relatively small and does not compromise the existence of differential left and right circularly polarized light absorption. Considering these findings, although Fig. 3b and c reveal the presence of long tails on the right side of the CD bands, which are indicative of differential scattering of the

incident light, the observed large CD bands should be mainly due to light absorption processes. Nevertheless, both differential left- and right-circularly polarized light absorption and differential left- and right-circularly polarized light scattering have been associated with long-range chiral structures.[46] Consequently, in the present case, the large bands in the CD spectra of DNA/dendrimer films should be a manifestation of the formation of a supramolecular arrangement of the condensed DNA molecules (at least partially), resulting in a chiral system. Drawing a parallel with what happens with cholesteric liquid crystalline dispersions of DNA, right-handed superhelices should form inside the films, as the observed large CD bands are positive.[47] This long-range order was likely potentiated by the slow cooling program applied during film formation, which gave the system enough time for self-organization. Indeed, several studies report that dendrimers bind to DNA, bending the DNA helix and creating ordered mesophases containing DNA superhelices.[13,17,28,48–50] Mansel *et al.* referred to this phenomenon as "dendrimer-induced DNA superhelicity".[48] Interestingly, for our DNA/dendrimer films, although the DNA underwent a denaturation process (ssDNA formation) before contact with the dendrimers, superhelices were also generated after cooling. Possibly, there are ordered domains within the films formed by dendrimers and dsDNA (domains containing DNA superhelices) that are linked by dsDNA segments resulting from the random cross-hybridization of different DNA molecules *i.e.*, a crosslinked 2D material is formed that is partially crystalline.

While film formation seems to depend on the dendrimer's initial protonation state and the global proportion of positive and negative charges in solution, the extent of order achieved within the film appears to be generation-dependent (Fig. 3c). Possibly, G3 dendrimers are the most efficient at bending DNA, thus leading to films with CD signals of higher amplitude than those obtained with films made from G4 and G5 dendrimers. Indeed, research on the interaction between DNA and dendrimers has reported the formation of structures with different shapes (*e.g.*, rods, toroids, and beads-on-string) depending on the dendrimer generation used.[13,17,28,48–50] Therefore, it is not surprising that different generations of dendrimers also influence the characteristics of the formed films and impact CD signals. Moreover, the presence of a higher quantity of dendrimers in the film (higher N/P ratio) likely stabilizes the supramolecular structure formed. In this regard, films prepared with G3 dendrimers at an N/P ratio of 5 were those that achieved a higher degree of crystallinity. Interestingly, these films were also the ones that proved to be more physically resistant when manipulated.

(e) Surface morphology by scanning electron microscopy (SEM). The surface of the DNA/dendrimer-based films was analyzed by SEM after dehydration. All films exhibited identical surface morphology, regardless of the dendrimer generation and N/P ratio used in their preparation. Fig. 4 shows representative images obtained from DNA/G3 dendrimer films at an N/P

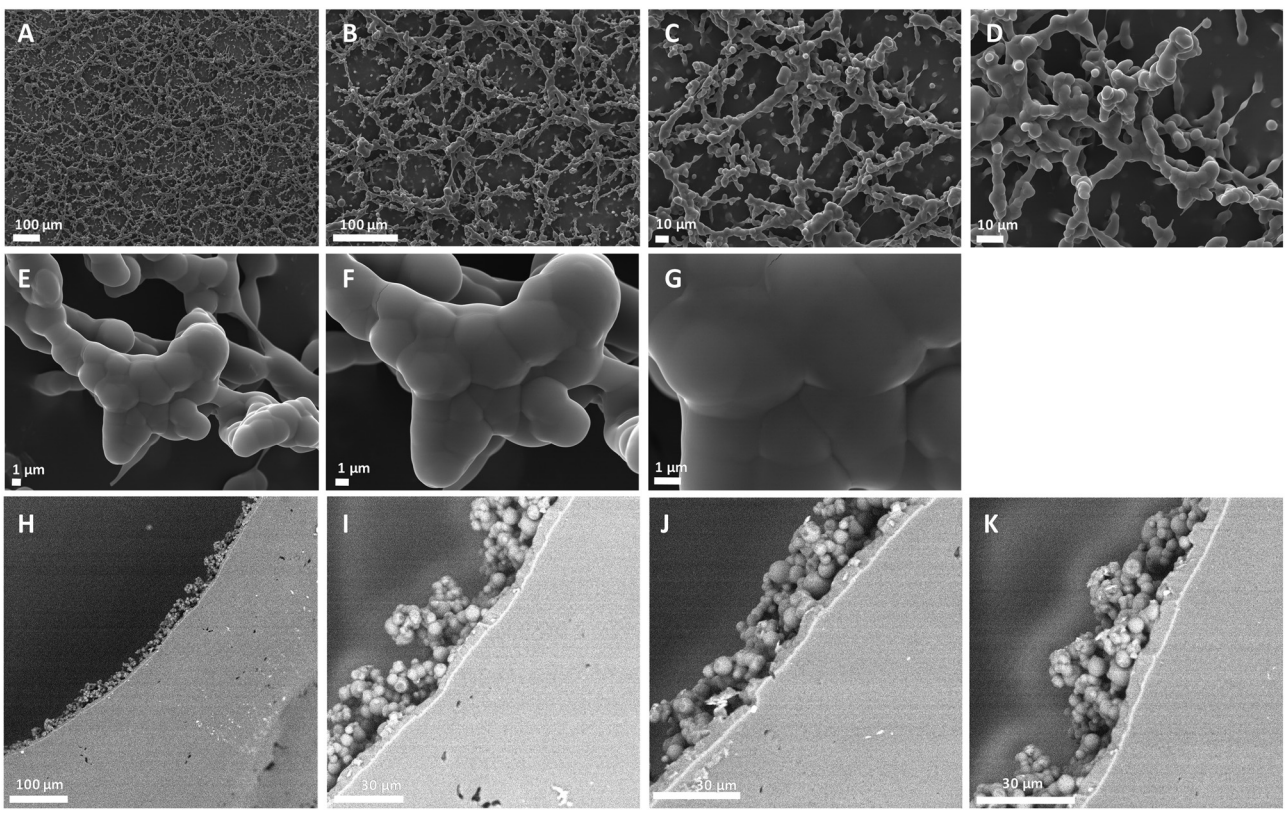

Fig. 4 Scanning electron microscopy images of dehydrated DNA/G3 dendrimer films prepared at the N/P ratio of 4. The top surface of the film that is in contact with the supernatant, at increasing magnifications from (A) to (G). The bottom surface of the film that is in contact with the flask surface, at increasing magnification, from (H) to (K).

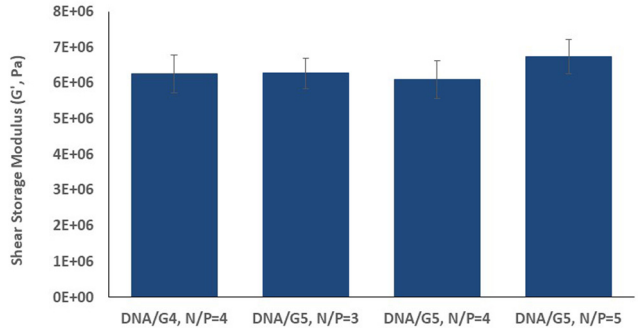

Fig. 5 The shear storage modulus (G') of air-dried DNA films (G4 at N/P = 4 and G5 at N/P = 3, 4, and 5). Results are presented as the mean ± s.d. (n = 3).

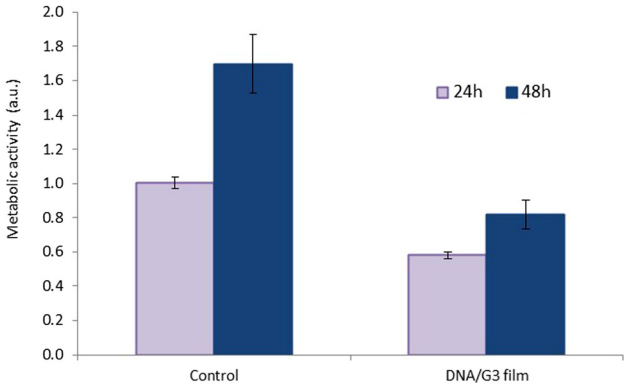

Fig. 6 Metabolic activity of NIH 3T3 cells cultured on the top of a DNA/dendrimer-based film prepared with G3 dendrimers at an N/P ratio of 4 after 24 and 48 h. Results are presented as the mean ± s.d (n = 4).

ratio of 4. Interestingly, the top surface of the films was composed of interconnected spherical particles (in the micrometer range), which were homogeneously distributed and consistent with the existence of an internal organization in the material. On the other hand, a smooth surface was observed when the bottom of the films was examined, revealing a compact and most likely amorphous material. It is possible that larger and less ordered DNA/dendrimer aggregates, having a higher sedimentation rate, were deposited at the bottom of the flask forming the more compact layer of the material (which may also be affected by adhesion forces established with the plastic/glass substrate and the film), while smaller DNA/dendrimer aggregates remained longer in the bulk solution, thus achieving a higher degree of internal organization (*i.e.*, forming DNA superhelices). Moreover, the integrity and continuity of the films were likely maintained through base pairing between segments of ssDNA from different molecules, either within each layer or between the two distinct layers of the material.

(f) Elasticity measurements. The shear storage modulus (G') of DNA/dendrimer-based films prepared with G4 and G5 dendrimers at different N/P ratios was measured (Fig. 5). Since the produced films rapidly lose water when exposed to air, which significantly affects the measurement of their mechanical properties, the G' analysis was performed on fully air-dried samples. The results showed that G' was in the range of 6×10^6–7×10^6 Pa, regardless of the dendrimer generation or the N/P ratio, indicating that the films behave like elastomers, efficiently storing mechanical energy when subjected to oscillatory shear stress (see also Fig. S8 in the ESI†).

(g) Cytocompatibility evaluation. With the potential biomedical applications of these films in mind, their cytocompatibility was evaluated. To this end, NIH 3T3 fibroblasts were directly seeded onto the surface of films prepared with G3 dendrimers at an N/P ratio of 4, and metabolic activity was assessed after 24 and 48 h (Fig. 6), along with cell visualization by optical microscopy (ESI,† Fig. S9). Results showed that the cells adhered to the films and proliferated over time, albeit to a lesser extent than in the control – an expected result because standard cell culture plastic is optimized for cell attachment. Overall, these experiments revealed that the films exhibit good cytocompatibility.

Scale-up of the films

Although the optimized protocol for film formation was established using microcentrifuge tubes and a thermoblock to control the temperature, the scaling up of films was shown to be possible using glass flasks with a progressively increasing flat-bottom surface area and a simple incubator (in this case, the temperature was varied from 100 °C to RT at a rate of 15 °C h^{-1}). Films readily formed at the bottom of the flasks (ESI,† Fig. S10). Their DNA content was controlled by adjusting the volume of the starting solutions, while their thickness was regulated by modifying the ratio between solution volumes and the deposition area. Thinner films exhibited a good level of transparency.

Conclusions and perspectives

In summary, novel DNA-based films were created using a heating/cooling process driven by electrostatic interactions between DNA and PAMAM dendrimers (G3 to G5), alongside the concurrent random base pairing of ssDNA segments. The preparation of these films required carefully optimized experimental conditions, and this study provided valuable insights into their nature. Circular dichroism analysis indicates that the films exhibit supramolecular chirality, while electron microscopy also points to the presence of ordered structures. Films were also found to be stable over time in nuclease-containing media and exhibited elastic behaviour when dehydrated.

We anticipate that films of this kind could find applications in biomedicine and biotechnology as drug or gene delivery systems, as platforms for *in vitro* cell-free DNA transcription, or in combination with DNAzymes for biosensing and diagnostic purposes.[51,52] Additionally, their supramolecular chirality could be harnessed for sensor development or the creation of novel 2D materials with unique chemical and physical properties through integration with other chemical entities, such as DNA intercalators, metallic ions, or various nanomaterials. Clearly, the strong interaction between PAMAM dendrimers and DNA suggests the possibility of creating countless new materials with interesting technological and biomedical applications.

Author contributions

The manuscript was written with contributions from all authors. All authors have approved the final version of the manuscript.

Data availability statement

The data supporting this article are included either in the main text or as part of the ESI.† The ESI† includes detailed experimental methods, additional figures/tables and a movie showing a film (i) being manipulated, (ii) prepared from fluorescently labelled dendrimers, (iii) stained with ethidium bromide and (iv) being degraded at high pH values.

Conflicts of interest

There are no conflicts of interest to declare.

Acknowledgements

This work was supported at CQM by the Portuguese Government through Fundação para a Ciência e a Tecnologia (FCT)/Ministério da Ciência, Tecnologia e Inovação (Base Fund: UIDB/00674/2020, DOI: 10.54499/UIDB/00674/2020; Programmatic Fund: UIDP/00674/2020, DOI: 10.54499/UIDP/00674/2020). R. Castro acknowledges FCT for the PhD grant (Ref. SFRH/BD/87465/2012). This work was supported at i3S by POCI-01-0145-FEDER-007274, as well as by the European Regional Development Fund (ERDF) through COMPETE 2020 – Operational Programme for Competitiveness and Internationalisation (POCI), Portugal 2020. Circular dichroism measurements were conducted at the Biochemical and Biophysical Technologies i3S Platform with the assistance of Frederico Silva (PhD), and zeta potential measurements were performed at the Biointerfaces and Nanotechnology i3S Scientific Platform, a member of the Portuguese Platform of Bioimaging (PPBI; PPBI-POCI-01- 0145-FEDER-022122), with the assistance of Ricardo Vidal (MSc). A. P. P. also acknowledges the MOBILIsE Project, which has received funding from the European Union's Horizon 2020 research and innovation program under grant agreement no. 951723. This study was also financed by project IBEROS+ (0072_IBEROS_MAIS_1_E, Interreg-POCTEP 2021-2027).

References

1 D. Astruc, E. Boisselier and C. Ornelas, *Chem. Rev.*, 2010, **110**, 1857–1959.
2 S. Mignani, J. Rodrigues, H. Tomas, M. Zablocka, X. Shi, A. M. Caminade and J. P. Majoral, *Chem. Soc. Rev.*, 2018, **47**, 514–532.
3 D. A. Tomalia and J. M. J. Fréchet, *J. Polym. Sci., Part A:Polym. Chem.*, 2002, **40**, 2719–2728.
4 D. A. Tomalia, A. M. Naylor and W. A. Goddard, *Angew. Chem., Int. Ed. Engl.*, 1990, **29**, 138–175.
5 D. A. Tomalia, H. Baker, J. Dewald, M. Hall, G. Kallos, S. Martin, J. Roeck, J. Ryder and P. Smith, *Polym. J.*, 1985, **17**, 117–132.
6 W. Chen, D. A. Tomalia and J. L. Thomas, *Macromolecules*, 2000, **33**, 9169–9172.
7 P. K. Maiti, T. Çağin, G. Wang and W. A. Goddard, *Macromolecules*, 2004, **37**, 6236–6254.
8 D. Pandita, J. L. Santos, J. Rodrigues, A. P. Pêgo, P. L. Granja and H. Tomás, *Biomacromolecules*, 2011, **12**, 472–481.
9 J. L. Santos, H. Oliveira, D. Pandita, J. Rodrigues, A. P. Pêgo, P. L. Granja and H. Tomás, *J. Controlled Release*, 2010, **144**, 55–64.
10 J. L. Santos, D. Pandita, J. Rodrigues, A. P. Pêgo, P. L. Granja, G. Balian and H. Tomás, *Mol. Pharmaceutics*, 2010, **7**, 763–774.
11 Y. Dong, T. Yu, L. Ding, E. Laurini, Y. Huang, M. Zhang, Y. Weng, S. Lin, P. Chen, D. Marson, Y. Jiang, S. Giorgio, S. Pricl, X. Liu, P. Rocchi and L. Peng, *J. Am. Chem. Soc.*, 2018, **140**, 16264–16274.
12 V. Leiro, A. P. Spencer, N. Magalhães and A. P. Pêgo, *Biomaterials*, 2022, **281**, 121356.
13 Y.-C. Huang, C.-J. Su, C.-Y. Chen, H.-L. Chen, U.-S. Jeng, N. V. Berezhnoy, L. Nordenskiöld and V. A. Ivanov, *Macromolecules*, 2016, **49**, 4277–4285.
14 K. Zhou, G. Gaullier and K. Luger, *Nat. Struct. Mol. Biol.*, 2019, **26**, 3–13.
15 S. Baldi, P. Korber and P. B. Becker, *Nat. Struct. Mol. Biol.*, 2020, **27**, 109–118.
16 C. A. Davey, D. F. Sargent, K. Luger, A. W. Maeder and T. J. Richmond, *J. Mol. Biol.*, 2002, **319**, 1097–1113.
17 R. Dootz, A. C. Toma and T. Pfohl, *Soft Matter*, 2011, **7**, 8343–8351.
18 M. Kéri, Z. Nagy, L. Novák, E. Szarvas, L. P. Balogh and I. Bányai, *Phys. Chem. Chem. Phys.*, 2017, **19**, 11540–11548.
19 K. Fant, E. K. Esbjörner, P. Lincoln and B. Nordén, *Biochemistry*, 2008, **47**, 1732–1740.
20 M. L. Örberg, K. Schillén and T. Nylander, *Biomacromolecules*, 2007, **8**, 1557–1563.
21 R. Owczarzy, B. G. Moreira, Y. You, M. A. Behlke and J. A. Wälder, *Biochemistry*, 2008, **47**, 5336–5353.
22 A. M. Naylor, W. A. Goddard, G. E. Kiefer and D. A. Tomalia, *J. Am. Chem. Soc.*, 1989, **111**, 2339–2341.
23 P. K. Maiti and B. Bagchi, *Nano Lett.*, 2006, **6**, 2478–2485.
24 B. Nandy and P. K. Maiti, *J. Phys. Chem. B*, 2011, **115**, 217–230.
25 C. S. Braun, J. A. Vetro, D. A. Tomalia, G. S. Koe, J. G. Koe and C. R. Middaugh, *J. Pharm. Sci.*, 2005, **94**, 423–436.
26 M. L. Ainalem and T. Nylander, *Soft Matter*, 2011, **7**, 4577–4594.
27 Y. Su, X. Quan, L. Li, J. Zhou, Y. Su, X. Quan, L. Li and J. Zhou, *Macromol. Theory Simul.*, 2018, **27**, 1700070.
28 K. Qamhieh, T. Nylander, C. F. Black, G. S. Attard, R. S. Dias and M. L. Ainalem, *Phys. Chem. Chem. Phys.*, 2014, **16**, 13112–13122.
29 L. B. Jensen, G. M. Pavan, M. R. Kasimova, S. Rutherford, A. Danani, H. M. Nielsen and C. Foged, *Int. J. Pharm.*, 2011, **416**, 410–418.

30 D. Fischer, Y. Li, B. Ahlemeyer, J. Krieglstein and T. Kissel, *Biomaterials*, 2003, **24**, 1121.
31 O. A. Ukogu, A. D. Smith, L. M. Devenica, H. Bediako, R. B. McMillan, Y. Ma, A. Balaji, R. D. Schwab, S. Anwar, M. Dasgupta and A. R. Carter, *Nucleic Acids Res.*, 2020, **48**, 6108–6119.
32 B. Scheicher, A. L. Schachner-Nedherer and A. Zimmer, *Eur. J. Pharm. Sci.*, 2015, **75**, 54–59.
33 I. Ruseska, K. Fresacher, C. Petschacher and A. Zimmer, *Nanomaterials*, 2021, **11**, 1508.
34 E. Bivehed, B. Hellman, Y. Fan, J. Haglöf and S. Buratovic, *Mutat. Res., Genet. Toxicol. Environ. Mutagen.*, 2023, **891**, 503680.
35 M. Liu, L. Zhang and T. Wang, *Chem. Rev.*, 2015, **115**, 7304–7397.
36 B. Ranjbar and P. Gill, *Chem. Biol. Drug Des.*, 2009, **74**, 101–120.
37 J. Kypr, I. Kejnovská, D. Renčiuk and M. Vorlíčková, *Nucleic Acids Res.*, 2009, **37**, 1713–1725.
38 M. Vorlíčková, I. Kejnovská, K. Bednářová, D. Renčiuk and J. Kypr, *Chirality*, 2012, **24**, 691–698.
39 I. Tinoco, M. F. Maestre, C. Bustamante and D. Keller, *Pure Appl. Chem.*, 1984, **56**, 1423–1428.
40 M. K. Cowman and G. D. Fasman, *Proc. Natl. Acad. Sci. U. S. A.*, 1978, **75**, 4759.
41 A. V. Pietrini and P. L. Luisi, *Biochim. Biophys. Acta, Biomembr.*, 2002, **1562**, 57–62.
42 M. F. Maestre and C. Reich, *Biochemistry*, 1980, **19**, 5214–5223.
43 Y. Yevdokimov, V. Salyanov, S. Skuridin, A. Dembo, Y. Platonov, A. Il'ina and V. Varlamov, *Dokl. Biophys.*, 2000, **374**, 47–49.
44 C. F. Jmdan, L. S. Lerman and J. H. Venable, *Nature, New Biol.*, 1972, **236**, 67–70.
45 Y. M. Yevdokimov, S. G. Skuridin, S. V. Semenov, L. A. Dadinova, V. I. Salyanov and E. I. Kats, *J. Biol. Phys.*, 2017, **43**, 45–68.
46 D. Keller and C. Bustamante, *J. Chem. Phys.*, 1986, **84**, 2972–2980.
47 S. V. Semenov and Y. M. Yevdokimov, *Biophysics*, 2015, **60**, 188–196.
48 B. W. Mansel, C. J. Su, C. Y. Chen, C. M. Young, Y. C. Huang, C. C. Yang and H. L. Chen, *Soft Matter*, 2021, **17**, 7287–7293.
49 C. Y. Chen, C. J. Su, S. F. Peng, H. L. Chen and H. W. Sung, *Soft Matter*, 2011, **7**, 61–63.
50 C. J. Su, H. L. Chen, M. C. Wei, S. F. Peng, H. W. Sung and V. A. Ivanov, *Biomacromolecules*, 2009, **10**, 773–783.
51 J. Yan, X. Ma, D. Liang, M. Ran, D. Zheng, X. Chen, S. Zhou, W. Sun, X. Shen and H. Zhang, *Nat. Commun.*, 2023, **14**, 1–21.
52 W. Ma, Y. Zhan, Y. Zhang, C. Mao, X. Xie and Y. Lin, *Signal Transduction Targeted Ther.*, 2021, **6**, 1–28.

